Energy Conversion and Management 67 (2013) 57–65

Contents lists available at SciVerse ScienceDirect

Energy Conversion and Management

journal homepage: www.elsevier.com/locate/enconman

Numerical study of the pressure drop phenomena in wound woven wire matrix of a Stirling regenerator

S.C. Costa [a,*], Harritz Barrutia [b], Jon Ander Esnaola [b], Mustafa Tutar [b,c]

[a] CS Centro Stirling S. Coop, Avda. Alaba 3, 20550 Aretxabaleta, Spain
[b] Mechanical and Manufacturing Department, Engineering Faculty of Mondragon University, Loramendi 4, 20500 Mondragon, Spain
[c] IKERBASQUE, Basque Foundation for Science, 48011 Bilbao, Spain

ARTICLE INFO

Article history:
Received 29 February 2012
Received in revised form 2 October 2012
Accepted 24 October 2012
Available online 12 December 2012

Keywords:
Stirling engine
Friction factor
Porosity
CFD
Laminar flow
Turbulence flow

ABSTRACT

Friction pressure drop correlation equations are derived from a numerical study by characterizing the pressure drop phenomena through porous medium of both types namely stacked and wound woven wire matrices of a Stirling engine regenerator over a specified range of Reynolds number, diameter and porosity. First, a finite volume method (FVM) based numerical approach is used and validated against well known experimentally obtained empirical correlations for a misaligned stacked woven wire matrix, the most widely used due to fabrication issues, for Reynolds number up to 400. The friction pressure drop correlation equation derived from the numerical results corresponds well with the experimentally obtained correlations with less than 5% deviation. Once the numerical approach is validated, the study is further extended to characterize the pressure drop phenomena in a wound woven wire matrix model of a Stirling engine regenerator for a diameter range from 0.080 to 0.110 mm and a porosity range from 0.472 to 0.638 within the same Reynolds number range. Thus, the new correlation equations are derived from this numerical study for different flow configurations of the Stirling engine regenerator. The results indicate flow nature and complex geometry dependent friction pressure drop characteristics within the present Stirling engine regenerator system. It is believed that the developed correlations can be applied with confidence as a cost effective solution to characterize and hence to optimize stacked and woven Stirling engine efficiency in the above specified ranges.

© 2012 Elsevier Ltd. All rights reserved.

1. Introduction

As it is widely known, Stirling engine technology presents high potential for energy cogeneration applications due to its elevate global efficiency, higher than 90%, and the possibility to operate with any high temperature heat source (solar, combustible material, field waste, biomass, nuclear, etc.) and low noise and contamination levels [1–5]. The regenerator is the most vital component of a Stirling cycle machine and most of the research works in this field have been focused on the characterization and optimization of the performance of this component in order to achieve such high efficiency [6–10]. Especially focused on cogeneration applications of Stirling engines, pressure losses through the regenerator have a direct influence on the engine indicated power and, consequently, on the obtained electric power [8–10]. Therefore, the characterization of this phenomena through experimental, theoretical and numerical studies is crucial in those applications to maximize the incoming outsource energy to generated electric power transformation ratio.

Although there are different types of regenerators, the most widely used type is the stacked woven wire screen regenerator. Thus, most of the research works carried out about the fluid characterization in the Stirling regenerator have been focused especially in the empirical characterization of the pressure loss of this type of component. Frequently, the regenerator flow is modeled as an internal flow conduct using the law of Poiseuille. This model is widely used to compute the pressure loss as there are several correlations to determine the friction coefficient C_f. The correlation obtained by Kays and London [11], based on the incompressible flow hypothesis, is probably the most widely used one. It was obtained from experiences in perfectly pressed stacked wire screen matrices. The original Kays and London chart consists of four similar curves corresponding to the porosities of 0.602, 0.725, 0.766 and 0.832 respectively. Urieli and Berchowitz [12] proposed a correlation equation based on Kays and London data.

Seume and Simon [13] provide further review of the friction factor correlations for steady-state flow, and they also study the

* Corresponding author. Tel.: +34 943 037 948; fax: +34 943 792 393.
E-mail address: ccosta@centrostirling.com (S.C. Costa).

0196-8904/$ - see front matter © 2012 Elsevier Ltd. All rights reserved.
http://dx.doi.org/10.1016/j.enconman.2012.10.014

Nomenclature

a_1	resistance form parameter	S_{ij}	strain-rate tensor
a_2	surface friction parameter	μ	fluid viscosity
a_3	friction coefficient equation parameter	μ_t	turbulent viscosity
C_f	friction coefficient	ρ	fluid density
d_h	matrix diameter hydraulic	Π_v	matrix volumetric porosity
d_w	wire diameter	ϕ	matrix shape factor
L	length of the matrix	τ_{ij}	Reynolds stress tensor
ΔP	pressure drop	k	turbulence kinetic energy
Re	Reynolds number	ε	dissipation rate for the turbulence kinetic energy
u_{max}	matrix velocity		
u_1,u_2	time averaged velocity components		

compressibility effects and the oscillating characteristics of the thought Stirling engine regenerators. Sodré and Parise [14] carried out experiments to determine the pressure drop through an annular conduit filled with a plain square wire-mesh woven-screen matrix. A corrected Ergun equation [15] was used to correlate the experimental data, considering wall effect.

Miyabe et al. [16] derived generalized experimental equations of flow friction factor and heat transfer coefficient for packed wire screens with variety of geometries. Tanaka et al. [8] investigated the flow and heat transfer characteristics of the regenerator materials in an oscillating flow for wire net and sponge metal. The prediction of pressure drop loss was possible by use of the hydraulic diameter as the representative length defined by the friction factor and Reynolds number. Gedeon and Wood [17] derived generic correlations for friction factor, Nusselt number, enhanced axial conduction ratio and overall heat flux ratio based on the test samples of a number of wire mesh and metal felt, with a range of porosities.

Thomas and Pittman [18] compared different research pressure drop correlations and pointed out that the pressure drop caused by the flow through an array of wires is mainly affected by two mechanisms: the resistance form (a_2) and the surface friction (a_1). This means that the correlation form (Eq. (1)) is based on the well-know Ergun equation [15]. Roughly, the Ergun equation [15] implies creeping-viscous-dominated Darcy flow for low Re, where a_1/Re dominates, smoothly transitioning to turbulence-like flow at high Re, where (a_2) dominates.

$$C_f = (a_1/Re) + a_2 \quad (1)$$

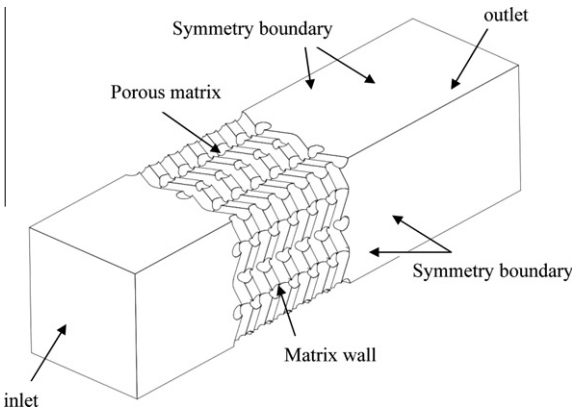

Fig. 1. Global computational domain for stacked woven wire matrix.

Apart from the analytical studies, there are some numerical analyses of the flow through wire screen matrix conducted with use of different numerical discretization techniques. The finite volume method (FVM) appears to be promising as indicated by Rühlich and Quack [7], Gedeon and Wood [17], Ibrahim et al. [9,20], Tew et al. [19] and others. These numerical studies suggest that the flow simulation is highly required to understand the flow of interest and hence to characterize fluid flow friction behavior for such systems of regenerator applications.

As summarized above, the majority of experimental studies and correlations have been generally conducted for stacked wo-

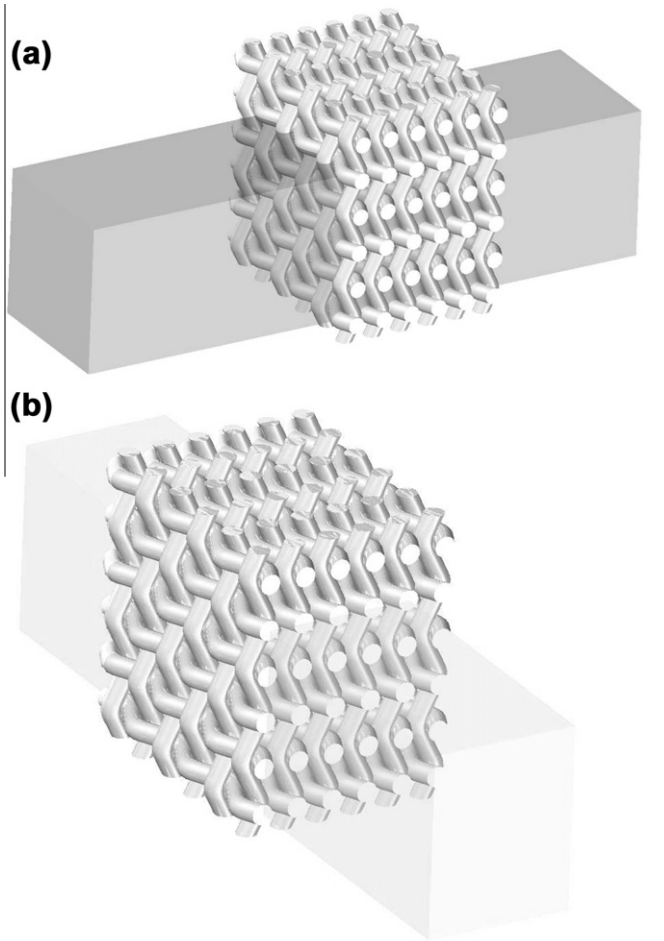

Fig. 2. Woven wire matrix configuration: (a) stacked woven wire matrix configuration; and (b) wound woven wire matrix configuration.

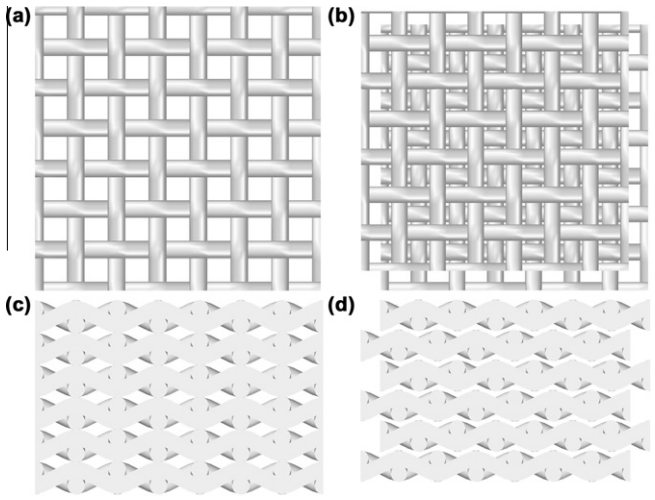

Fig. 3. 2-D flow perpendicular plane layouts: (a) staked aligned; (b) stacked misaligned; (c) wound aligned; and (d) wound misaligned cases.

ven wire screen regenerator matrices as they are the most widely used ones. However, this kind of regenerator tends to be the one of the most expensive components of the Stirling engines [21], being the price one of the disadvantages which nowadays limit the use of this technology for micro-cogeneration application in domestic environments. For this reason, the use of wound woven wire matrix regenerators could be a more cost effective alternative solution that could overcome such limitations. Even though, very few research works have been carried out for this type of regenerator, there is still no specific pressure drop correlations are known to exist in literature. Thus, there is still the necessity to characterize the pressure drop phenomena in this type of regenerator.

Therefore, this study mainly focuses on the development of numerically obtained correlations to determine pressure losses through a wound woven matrix regenerator for different configurations. With this respect, numerical models for a stacked woven wire matrix are initially developed to obtain pressure drop correlations for different configurations and the results are compared with well-known experimentally obtained correlations in order to validate the proposed models over a specified range of *Re* number. Later, the numerical study is extended to obtain pressure drop friction factor correlation equation for wound woven wire matrices at different configurations. The good correspondence of the stacked case with experimental data suggests that the derived correlations can be used with confidence to characterize and hence to optimize wound woven Stirling engine efficiency by avoiding expensive try and error experimental tests. However, it is expected that the developed correlations be experimentally validated in future work.

Concerning modeling of flow physics, a stepwise approach is followed here with increasing complexity, starting with stationary and isothermal flow computations with adiabatic wall boundary conditions and progressing to the transient (time-dependent), non-isothermal flow computations concerning heat transfer effects on pressure drop characteristics. As a first step of numerical optimization of pressure losses in Stirling engine Regenerator, in this study a three-dimensional (3-D) isothermal simulation with an initial flow field is proposed for determining pressure drop characteristics, thus providing a straightforward insight in how to determine frictional losses at different geometric configurations at different *Re* values with generalized pressure drop correlation equations derived from a CFD approach. Since the characteristic streamwise dimension of the matrix domain (around 1 mm) is not also large with respect to the computational domain length, the temperature effects are not considered to be significant for this first attempt computations.

2. Computational principles

2.1. Numerical methodology

In the present numerical study, the fluid is considered to be viscous, incompressible, Newtonian, and 3-D with assumption of laminar flow behavior at very low Reynolds number range and of turbulent flow behavior at high Reynolds number. As the Reynolds number exceeds a certain value depending on the configuration of the wire matrix used, the local instabilities due to emergence of turbulence lead to numerical convergence problem and the simulations are conducted in turbulent manner. The present flow is mathematically governed by continuity equation and momentum equation, known as Navier–Stokes equations, which are derived from the basic concept of conservation laws of mass and momentum, respectively. Since there is no known analytical solution, or direct mathematical representation, these governing equations are discretized and solved sequentially using a finite volume method (FVM) based numerical flow solver [22] with a second order upwind scheme for the discretization of the continuity and momentum equations for the laminar flow solutions. All fluid properties—including density, viscosity are assumed to be constant. The convergence criterion for all the velocity and pressure components and for the continuity is set to 10^{-6} to attain high numerical accuracy.

2.2. Computational domain

Fig. 1 illustrates the region of flow of interest (geometry set-up) in which the flow through woven wire matrix geometry is extensively analyzed as a representation of a differential part of a Stirling regenerator arrangement. The inlet and outlet flow areas are set to 1 mm^2.

The hydraulic diameter based Reynolds number is varied from 10 to 400. In some simulations the computational domain is further extended in the downstream direction (in the nominal direction of the outlet flow) in order to avoid reverse flow conditions at the outflow boundary.

Two different configurations, perfectly aligned and misaligned, for each woven wire matrix, stacked wire and wound woven wire, are generated and studied. Furthermore, for same aligned and mis-

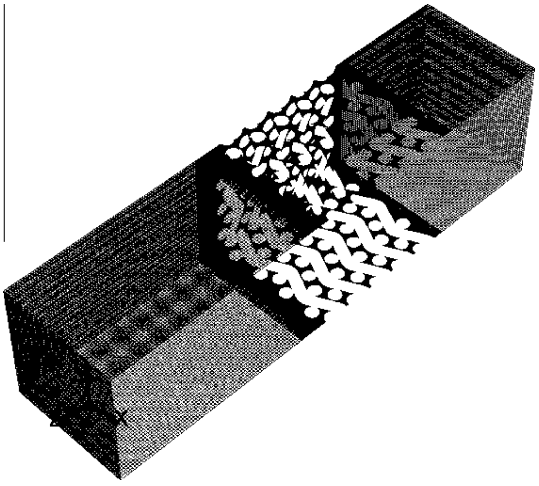

Fig. 4. 3-D view of the grid layout for the computational domain.

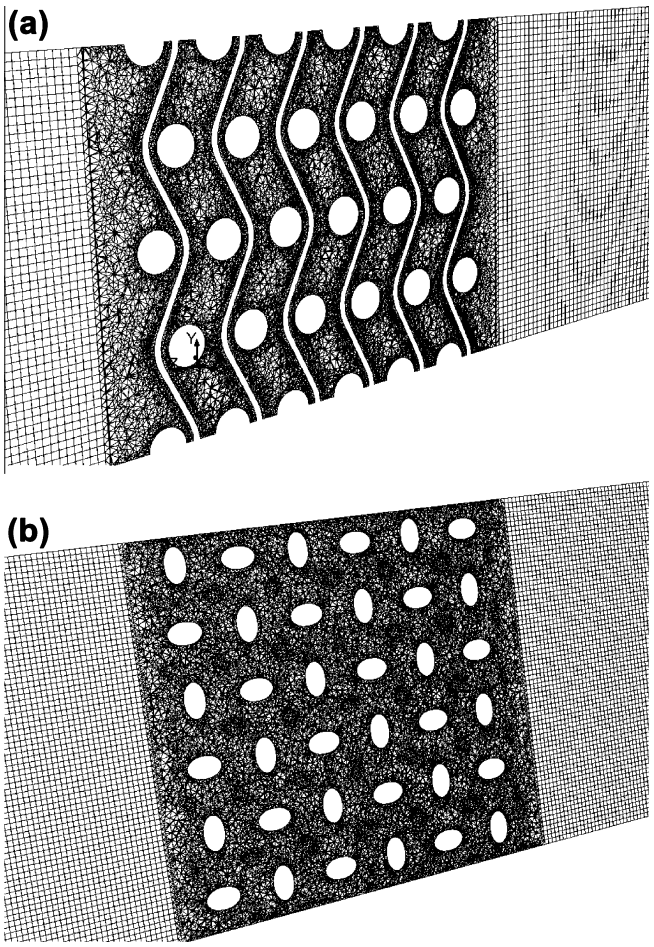

Fig. 5. 2-D plane view of woven wire flow matrices for two different configurations; (a) stacked woven mesh configuration; and (b) wound woven mesh configuration.

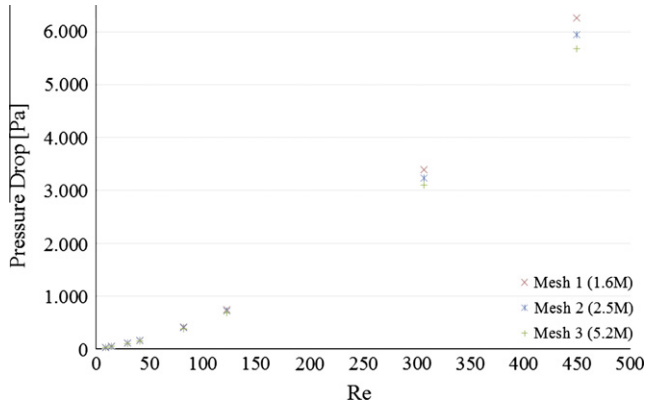

Fig. 6. Mesh sensibility for different number of volume cells: pressure drop vs. *Re*.

aligned levels, different volumetric porosity rages, Π_v, from 0.387 to 0.641 are also taken into consideration. Fig. 2a and b shows the flow direction for a perfectly aligned local matrix for stacked and wound woven models, respectively.

Fig. 3a–d shows 2-D flow perpendicular plane layouts for perfectly aligned and misaligned configurations for both, stacked and wound woven cases.

3-D view of the grid layout for the computational domain is represented in Fig. 4 and 2-D sections of two planes in the flow direction are also provided for two different configurations in Fig. 5. The computational domain is constructed of non-uniformly distributed different hybrid mesh systems with over 2.5 million tetrahedral and/or hexahedral volume cells for the final mesh system. The tetrahedral cells are used in the air volume inside the matrix with very fine mesh resolution in the close vicinity of the wire surfaces to resolve sharply varying velocity and pressure gradients there. As the accuracy of the present numerical results may depend on the mesh resolution in the computational domain, the effect of the mesh resolution on the present flow is initially tested through a grid independence study for three different mesh systems containing non-uniformly distributed hybrid grid cells (from 1.5 million to 5 million volume cells). As seen in Fig. 6, although the discrepancy among pressure drop values obtained from different mesh configurations becomes larger as the flow velocity increases, there is no major difference among the computed values and the mesh system of over 2.5 million hybrid volume cells. Thus, it could be considered to be fine enough to study the effects of Reynolds number on the pressure drop characterization through subsequent flow simulations.

All calculations are carried out on a PC cluster system with configuration of Intel Xeon CPU X5680 of four nodes parallel processors running at 3.33 GHz each on 72 GB RAM memory and typically each simulation takes about 3 days, 5.5 days and 13.3 days of CPU to converge for meshes containing 1.6 million, 2.5 million, and 5.2 million grid cells, respectively.

2.3. Boundary conditions

For all woven wire matrix configurations, all model simulations are carried out by considering the following boundary conditions:

1. Velocity inlet boundary conditions: velocity inlet boundary conditions are used to define the fluid uniform velocity profile at the inlet.
2. Pressure outlet boundary conditions: pressure outlet boundary conditions are used to define the static (gauge) pressure at the outlet boundary and to eliminate reverse flow problem.
3. Symmetry boundary conditions: free-slip boundary conditions at the four side boundaries of the computational domain are imposed. The normal velocity components and the normal gradients of all velocity components are assumed to have a zero value.
4. Interior wall boundary conditions: no-slip wall boundary conditions together with the standard wall functions are used to define the interior wall boundaries between wires and flow for turbulent simulation cases.

2.4. Laminar vs. turbulent flow analysis

In the present study, after a certain value of defined *Re* number (approximated *Re* number of 160), there may be emergence of local turbulence instabilities leading to convergence problem for laminar flow simulations as shown in Fig. 7b. The comparative presentation of residual statistics for each conserved variable i.e. continuity and three-velocity components, indicates that the convergence history exhibits significant oscillatory behavior for each residual starting with *Re* number of 160 as shown in Fig. 7b while the convergence history of residuals at *Re* number of 150 exhibits rather smooth convergence rate as shown in Fig. 7a. Therefore, it can be concluded here that *Re* number of 160 could represent a threshold value from laminar to turbulent transition for the present flow system. Hence it has to be resolved or modeled by a turbulence model to accurately predict the pressure drop values at high Reynolds numbers after *Re* number of 160. This local transitional characteristic change in the flow of different regenerators has been also previously investigated and well documented.

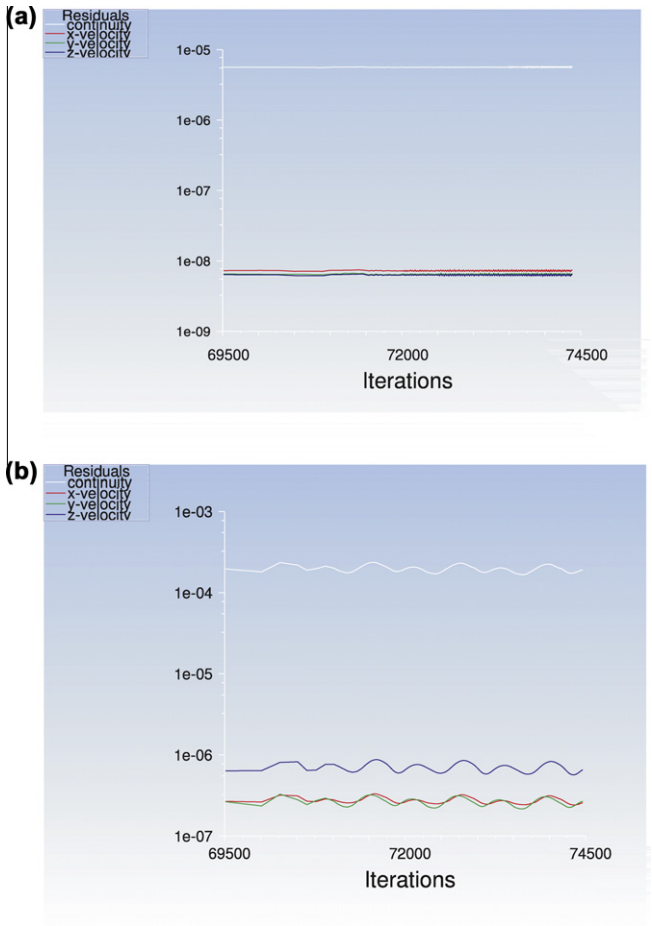

Fig. 7. The convergence history for residuals for a woven wire flow matrix at different *Re* numbers; (a) *Re* number of 150; and (b) *Re* number of 160.

Seume and Simon [13] studied the type of flow regime in the regenerator of different engines, the characteristic Reynolds numbers are low between 60 and 350, despite which the flow regime is not always laminar. Dybbs and Edwards [23] classified the steady flow regimes in porous media according to a Reynolds number based on the average pore diameter: $Re < 1$ Darcy flow regime; $1 < Re < 10$ boundary layers begin to develop on the pore wall, $10 < Re < 175$ laminar flow, $175 < Re < 250$ separated laminar flow, vortex shedding, $250 < Re < 300$ separated flow with random wakes and $Re > 300$ turbulent flow.

The complex and irregular geometry of the present porous media makes the 3-D flow resolution difficult and the associated pressure drop predictions may become inaccurate. Therefore, for $Re > 175$ for stacked woven wire matrix and for $Re > 230$ for wound woven wire matrix configuration with use of laminar model computations, there may be a requirement of using turbulence model to accurately represent the local turbulence and their effects on prediction of pressure drops. With this respect, turbulence is modeled here using Reynolds averaged Navier–Stokes (RANS) equations based RNG k–ε turbulence model which was originally developed by Yakhot and Orszag [24] to account for the effects of smaller scales of motion to improve the capabilities of the standard k–ε model for flows in which highly swirling patterns and separation prevail.

The forms of the k and ε equation of the RNG k–ε model are then given as follows:

$$u_j \frac{\partial k}{\partial x_j} = \frac{\partial}{\partial x_j}\left(\frac{\nu_t}{\sigma_k}\frac{\partial k}{\partial x_j}\right) + \nu_t\left(\frac{\partial \bar{u}_i}{\partial x_j} + \frac{\partial \bar{u}_j}{\partial x_i}\right)\frac{\partial \bar{u}_i}{\partial x_j} - \varepsilon \tag{2}$$

$$u_j \frac{\partial \varepsilon}{\partial x_j} = \frac{\partial}{\partial x_j}\left(\frac{\nu_t}{\sigma_\varepsilon}\frac{\partial \varepsilon}{\partial x_j}\right) + C_1\frac{\varepsilon}{k}\nu_t\left(\frac{\partial \bar{u}_i}{\partial x_j} + \frac{\partial \bar{u}_j}{\partial x_i}\right)\frac{\partial \bar{u}_i}{\partial x_j} - C_2\frac{\varepsilon^2}{k} - R \tag{3}$$

The coefficients C_1, C_2, C_μ, σ_k, σ_ε are constants in the sense that they are not changed in any calculation. The turbulence dissipation, ε equation of the RNG k–ε model includes the sink term, R to account for the different scales of motion through changes to the production term. Yakhot and Orzag [24] recommend the values of these values for these model coefficients are 0.085, 1.410, 1.680, 0.717, 0.717 and 0.387, respectively.

In the present study, the use of RNG k–ε model ensures that not excessively higher turbulent viscosities upstream of the stagnation region in the woven wire matrix domain leading to inaccurate flow predictions are observed in the flow domain in comparison with the standard k–ε model and its functionality has been previously proved for bluff body flows [25]. The present model is also employed with a medium level of inflow turbulence intensity with the inlet viscosity ratio $\mu_t/\mu < 10$ with 1% of the characteristic length scale (matrix dimension here) to make sure that the skin-friction can not deviate significantly from the laminar value.

3. Results and discussion

3.1. Numerical validation: pressure drop correlation for stacked woven wire matrix

In this section, the numerical simulations are performed using a proposed FVM method based numerical solution for the stacked woven wire matrix and a pressure drop friction factor correlation equation is derived from the results of the simulation to fit in comparison with the results of Tanaka et al. [8] and Gedeon and Wood [17] over a range of wire diameter, *Re* number and porosity as summarized in Table 1.

Tanaka et al. [8] and Gedeon and Wood [17] obtain friction coefficient correlations based on experimental oscillating flow. For this reason those correlations are considered for the validation of the numerical model presented for the study of stacked woven wire matrix regenerator.

Tanaka et al. [8] investigated the flow and heat transfer characteristics of regenerator materials in an oscillating flow for conventional stacked woven wire matrix, sponge metal (felt) and sintered metal. The prediction of pressure drop loss was possible by use of the hydraulic diameter as the representative length defined by the friction factor and Reynolds number. Tanaka et al. [8] observed that the wire diameter is not suitable as the representative length for various porosities and mesh shape. Tanaka et al. [8] observed that the friction factor in oscillating flow is about 30% higher than the theoretical value of unidirectional flow.

Gedeon and Wood [17] obtained correlations for friction factor, Nusselt number and other parameters for stacked and sintered woven wire matrices, and metal felt test regenerator samples. In pre-

Table 1
Tanaka et al. [8] and Gedeon and Wood [17] experimental range for stacked woven wire matrix and experimentally obtained empirical correlations for frictional pressure coefficient.

	Wire diameter (μm)	Porosity	*Re* range	Correlation
Tanaka et al. [8]	50–230	0.645–0.754	10–2000	$C_f = 175/Re + 1.60$
Gedeon/Wood [17]	53–94	0.623–0.781	0.45–6100	$C_f = 129/Re + 2.91Re^{-0.103}$
Present study	80–110	0.387–0.641	1–400	$C_f = 123/Re + 3.20Re^{-0.104}$

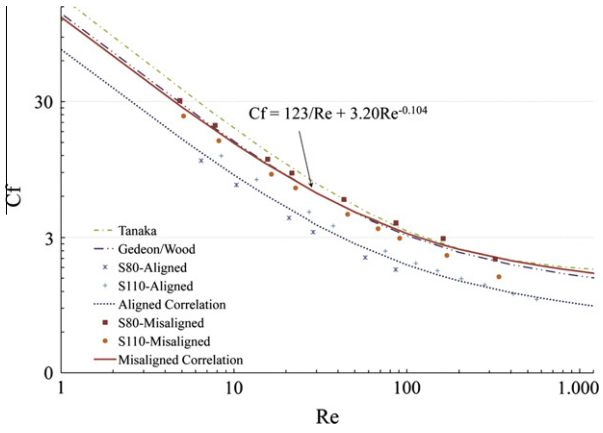

Fig. 8. Stacked woven wire matrices: friction factor vs. Reynolds number.

Table 2
Principal parameters deviation for calculated C_f values from Gedeon and Wood [17].

Parameters	Correlation	Min.% deviation	Max.% deviation	Avg.% deviation
a_1	$C_f = 123/Re + 2.91Re^{-0.103}$	0.4	4.6	2.6
a_2	$C_f = 129/Re + 3.20Re^{-0.103}$	0.0	9.1	4.5
a_3	$C_f = 129/Re + 2.91Re^{-0.104}$	0.0	0.6	0.2

vious investigations they concluded that there was no significant difference in heat-transfer or pressure drop characteristics produced by sintering compare to cold stacking (random orientation). Gedeon and Wood [17] started the modeling friction factors with the standard two-parameter Ergun form (Eq. (1)), but this equation showed a better fit to data by introducing a relatively minor modification to the Ergun equation [15], that they call three-parameter modified-Ergun form:

$$C_f = a_1 Re + a_2 Re^{a_3} \tag{4}$$

The parameter a_3 will be negative but allowing the correlations to better track at high Re, at low Re the a_1/Re will dominate, exactly as the original Ergun equation [15]. In addition, they introduced the matrix porosity as a parameter in the Ergun equation [15]; unfortunately that expression did not seem to fit the data very well. Even without explicit porosity dependence, porosity does affect the calculation of the hydraulic diameter d_h and maximum flow velocity $u_{\max}$ in terms of which friction factor was defined. The error of the combined correlation proposed by them to a generic woven wire matrix is 10%.

In both studies the maximum Reynolds number is calculated based on hydraulic diameter, d_h instead of wire diameter. The hydraulic diameter is defined as:

$$d_h = 4\Pi_v/\phi(1-\Pi_v) \tag{5}$$

where Π_v is the volumetric porosity and ϕ is the shape factor defined as the ratio of the mesh surface area to the mesh volume. Therefore, Reynolds number can be given as:

$$Re = \rho u_{\max} d_h/\mu \tag{6}$$

The maximum flow velocity $u_{\max}$ is obtained by dividing the frontal maximum velocity by porosity. The pressure drop is then defined as follows:

$$\Delta P = C_f \frac{\rho}{2}\frac{L}{d_h} u_{\max}^2 \tag{7}$$

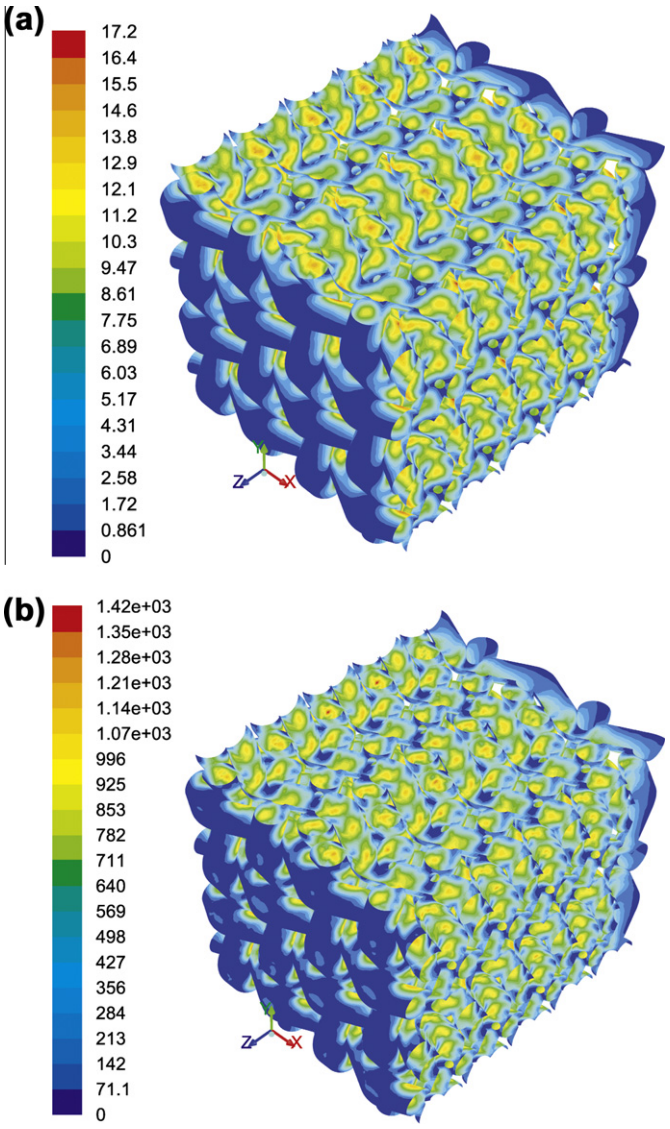

Fig. 9. Friction coefficient contours obtained for the wall surfaces of the matrices for the stacked woven wire misaligned matrix ($\Pi_v = 0.387$) domain at different inflow velocities; (a) $Re = 5$ ($u_{in} = 0.45$ m/s); (b) $Re = 170$ ($u_{in} = 15.00$ m/s).

Although the purpose of the present study is to estimate the pressure drop in a wound woven wire matrix, since there is no experimental data available for this case, the first step is to validate the computational model for a stacked woven wire matrix in comparison with the experimentally obtained empirical correlations proposed by cited researchers above. The validation is made using two wire diameters and two configurations of matrices in which, the first configuration is a stacked woven wire screens perfectly aligned and the second matrix configuration is with the maximum misalignment between them. In Table 1 the parametric study range for stacked woven wire matrices is summarized.

Tanaka et al. [8] proposes the following empirical relationship:

$$C_f = 175/Re + 1.60 \tag{8}$$

Gedeon and Wood [17] suggest the following three-parameter friction factor correlation:

$$C_f = 129/Re + 2.91Re^{-0.103} \tag{9}$$

In Table 1 are the empirical correlations coefficients for Tanaka et al. [8], Gedeon and Wood [17] and the present study for stacked woven wire screens.

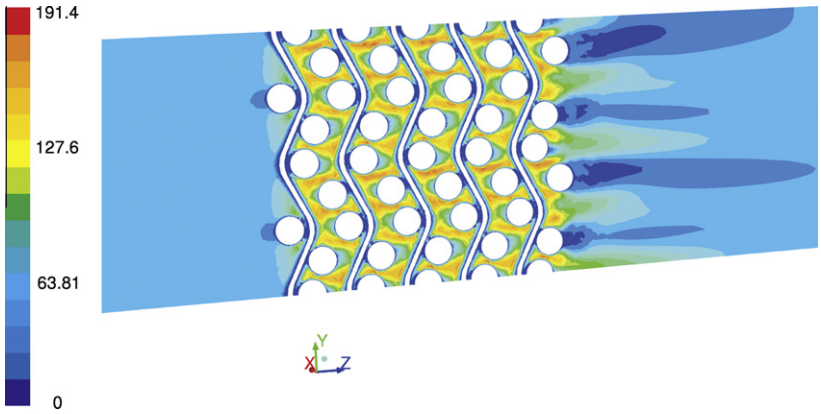

Fig. 10. Velocity magnitude contours on the mid-span plane of the flow domain at $Re = 238$ ($u_{in} = 15.00$ m/s) for the stacked woven wire misaligned matrix.

Table 3
Summary of model simulations performed for the wound woven wire matrix model.

Model	W1	W2	W3	W4	W5	W6	W7	W8	W9
d_w (mm)[a]	0.080	0.080	0.080	0.110	0.110	0.110	0.110	0.110	0.110
Misalignment (%)[b]	50	75	100	100	100	100	50	0	50
Π_v[c]	0.638	0.638	0.638	0.616	0.533	0.472	0.588	0.632	0.629

[a] d_w: wire diameter.
[b] Misalignment: displacement between woven wire screen layer perpendicular to flow direction, 100% represent maximum displacement.
[c] Π_v: volumetric porosity.

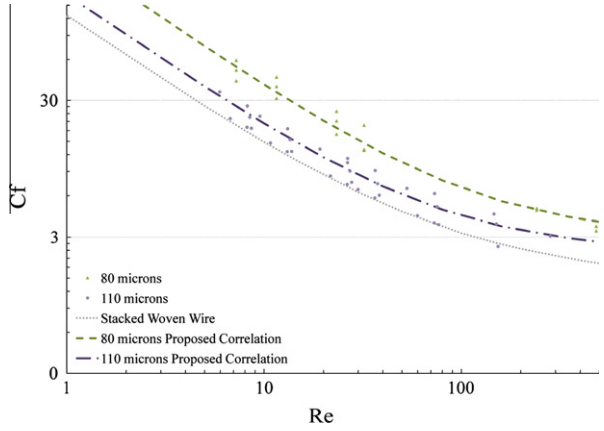

Fig. 11. Wound woven wire matrices: friction factor vs. Reynolds number.

Table 4
Model coefficients determined for C_f correlation for two different wire mesh diameters.

d_w (μm)	a_1	a_2	a_3
80	358	3.53	−0.018
110	176	2.84	−0.026
80–110	843.330–6.067 d_w	5.370–0.023 d_w	0.003–2.667E−4 d_w

Based on the pressure drop simulation results for four stacked woven wire matrices, the friction coefficient is calculated for each Reynolds number value. By fitting these results to the three-parameter Ergun equation form, a pressure drop friction factor correlation is obtained.

Fig. 8 shows the relationship between friction factor and Reynolds number for the experimental correlations due to Tanaka et al. [8] and Gedeon and Wood [17] (Eqs. (8) and (9)) and the friction factor obtained from the present results. It is observed that the friction coefficient obtained from the misaligned matrix show a good correspondence with Gedeon and Wood [17] correlations with less than 5% deviation for low Re range. When the present stacked wire model is further extended to analyze the pressure drop for a perfectly aligned configuration, 30% lower pressure drop values are observed compared to the misaligned case. Thus, the perfectly aligned ideal configuration can be considered to be the most appropriate solution from the efficiency point of view, even if it is hardly achievable by conventional manufacturing processes.

Based on the results from the three-parameter equation, the pressure drop friction correlation equation for the misaligned configuration can be derived as in the following equation, where the Reynolds number (Re up to 400) is calculated based on the hydraulic diameter:

$$C_f = 123/Re + 3.20Re^{-0.104} \quad (10)$$

Based on three-parameter comparison with that of Gedeon and Wood [17], for the summarized test conditions in Table 2, it is observed that the main deviation of calculated C_f values from those of Gedeon and Wood [17] is due to change in values of the principal parameters a_1 (reproduces 4.6% maximum deviation) and a_2 (reproduces of 9.1% maximum deviation). It can be noted here that a_1 is responsible for the surface friction effect at low Re number while a_2 is responsible for the friction resistance form due to increasing local turbulence effects at higher Re number.

The overall static pressure drop for the present flow problem is mainly governed by the form drag and the skin friction due to wall shear stress at the matrix walls. Thus, the local distribution of the skin friction on the matrix walls demonstrate its significant effects in the determination of the skin friction dependent pressure losses in the flow domain of the stacked woven misaligned matrix configuration in Fig. 9a and b. As seen in those figures, the walls of the woven wire matrices are the main sources of the skin friction coefficient and its magnitude increases as the Re number increases. In addition, almost similar local skin friction distributions are obtained for each case. The velocity contours in the mid-span plane of the flow domain (Fig. 10) also signifies the importance of local

increase of velocity magnitudes within the matrix domain as an indication of shear gradients leading to higher wall shear stress and hence friction pressure drops there in comparison with the rest of the flow domain.

3.2. The friction factor correlation for wound woven wire matrix

Once validated and used to derive the friction factor correlation as given in Eq. (10), the present numerical approach is extended to analyze the flow through a stacked woven wire matrix configuration. Table 3 summarizes all the parametric conditions studied for different wound woven wire matrix cases here.

Fig. 11 shows the relationship between friction factor and Reynolds number for the wound woven wire matrix simulations and the solid line present the friction factor correlation line derived from the present results for the investigated flow parameters' range. It is found that the average friction factor coefficients obtained for wound woven wire matrix are significantly greater than those obtained from the stacked woven case at low Reynolds numbers (<100), but for high Reynolds numbers both factors tend to be the same.

Considering that the woven wire matrix winding process is not easily controllable in regard to the alignment of different layers, the approach of an average ratio of the different cases are considered appropriated. The initial objective of the study is to derive a general pressure drop correlation equation based on *Re* number for wound woven wire mesh regenerator, in order to easily evaluate the pressure drop phenomena through a wound woven wire mesh regenerator. However, the results show that wire mesh diameter has also a significant influence on pressure drop computations in addition to *Re* number values. Therefore, based on the results obtained, the wire diameter is introduced as a parameter in the correlation equation. The correlation equation that better fits with the results for wound woven wire matrix is shown in Eq. (11), where the Reynolds number (*Re* up to 400) is calculated based on the hydraulic diameter and the wire diameter is introduced in microns:

$$C_f = (843.330 - 6.067d_w)/Re + (5.370 - 0.023d_w)\ Re\ (0.003 - 2.667\mathrm{E} - 4d_w) \quad (11)$$

Moreover, two specific correlations for the studied wire diameter cases are obtained from the general correlation, Eq. (12) corresponds to wire diameter 0.080 mm and Eq. (13) to wire diameter 0.110 mm. Table 4 summarizes the correlations equations obtained in this study.

$$C_f = 358/Re + 3.53Re^{-0.018} \quad (12)$$

$$C_f = 176/Re + 2.84Re^{-0.026} \quad (13)$$

It is also important to emphasize here that the aim of this study is not analyze the effect of each different regenerator parameter on the pressure losses, as this procedure requires a highly extensive computational effort.

The skin friction coefficient contours (Fig. 12a and b) for the wound woven misaligned wire matrixes at different *Re* numbers are also provided to make a qualitative comparison between the low and high Reynolds number effects on the distribution of the skin friction and hence the friction pressure losses for the matrix configuration. The skin friction coefficient here is determined through the wall surfaces in the matrix domain with the computation of wall shear stress normalized by the inflow velocity based dynamic pressure. The similar trend of local skin friction coefficient for the matrix domain is obtained as that of stacked woven wire matrix i.e. the higher the *Re* number, the higher the skin friction coefficient.

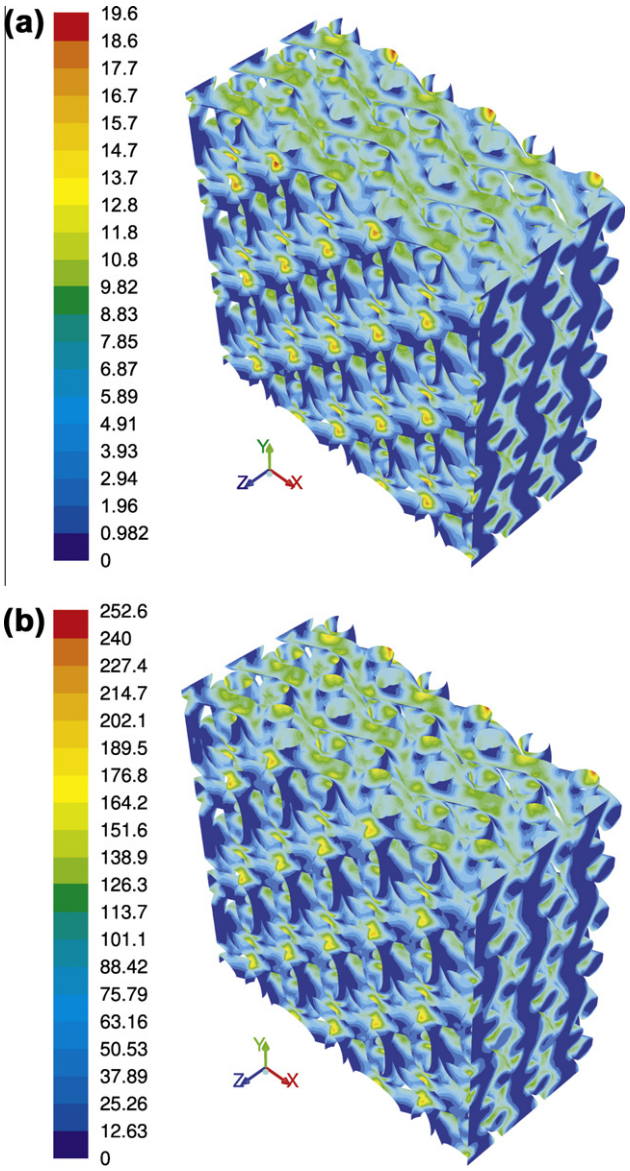

Fig. 12. Friction coefficient contours obtained for the wall surfaces of the matrices for the wound woven wire misaligned matrix domain at different inflow velocities; (a) $Re = 8$ ($u_{in} = 0.45$ m/s); and (b) $Re = 250$ ($u_{in} = 4.00$ m/s).

4. Conclusions

In the present numerical study, a universal correlation and two specific correlations are derived to characterize pressure drop friction factor for wound woven wire regenerator matrices following by an initial numerical validation against experimentally obtained correlation for stacked woven wire.

The validation results show that the derived correlation can be successfully applied in the *Re* number working range in Stirling regenerators ($Re < 350$), for diameter range from 0.080 to 0.110 mm and a porosity range from 0.472 to 0.638. The numerical study extended to wound wire model case also demonstrates an easy and effective use of the derived correlation for determining the pressure drop friction coefficient for the wound wire woven model for a large Reynolds number range up to 400. The numerical study results show a significant influence of the wire mesh diameter therefore two specific correlation parameters are proposed in other to reduce deviations.

It is believed that this new correlation can be also used with confidence as a cost effective tool to optimize pressure drop through this type of regenerator. Thus, by minimizing pressure losses, it is possible to maximize the indicated power and hence incoming outsource energy to generated electric power transformation ratio for cogeneration and micro-cogeneration applications. However, it is expected that the developed correlation be experimentally validated in the future.

The quantified comparative analysis between the stacked wire matrix system and the wound woven wire matrix system shows that even though the pressure drop for the wound woven matrices is higher than that of the stacked case, the present numerical tool can be used to improve wound wire matrix configuration by reducing the pressure losses and the cost of this component in the engine.

References

[1] Dorer V, Weber A. Energy and CO_2 emissions performance assessment of residential micro-cogeneration systems with dynamic whole-building simulation programs. Energy Convers Manage 2009;50(3):648–57.
[2] Formosa F, Despesse G. Analytical model for Stirling cycle machine design. Energy Convers Manage 2010;51(10):1855–63.
[3] Timoumi Y, Tlili I, Nasrallah B. Performance optimization of Stirling engines. Renew Energy 2008;33:2134–44.
[4] El-Ehwany AA, Hennes GM, Eid EI, El-Kenany EA. Development of the performance of an alpha-type heat engine by using elbow-bend transposed-fluids heat exchanger as a heater and a cooler. Energy Convers Manage 2011;52(2):1010–9.
[5] Zhong JH, Zheng YL, Li Q, Li Q. Evaluation of thermal efficiency and energy conversion of thermoacoustic Stirling engines. Energy Convers Manage 2010;51(4):802–12.
[6] Organ AJ. The regenerator and the Stirling engine. London: Mechanical Engineering Publications; 1997.
[7] Rühlich I, Quack H. New regenerator design for cryocoolers. Dresden (Germany): Technische Universität Dresden; 1999.
[8] Tanaka M, Yamashita I, Chisaka F. Flow and heat transfer characteristics of the stirling engine regenerator in an oscillating Flow. JSME Int J 1990;33(2):283–9.
[9] Ibrahim M et al. Improving performance of the Stirling converter: redesign of the regenerator with experiments. Computation and modern fabrication techniques. Cleveland State University; 2001.
[10] Andersen SK, Carlsen H, Thomsen PG. Numerical study on optimal Stirling engine regenerator matrix designs taking into account the effects of matrix temperature oscillations. Energy Conver Manage 2006;47:894–908.
[11] Kays WM, London AL. Compact Heat Exchangers 1984.
[12] Urieli I, Berchowitz DM. Stirling cycle engine analysis. Institute of Physics Publishing; 1984.
[13] Seume JR, Simon TW. A survey of oscillating flow in Stirling engine heat exchanger. NASA CR-182108; 1988.
[14] Sodré JR, Parise JAR. Friction factor determination for flow through finite wire-mesh woven-screen matrices. ASME J Fluids Eng 1997;119:847–51.
[15] Ergun S. Flow through packed columns. Chem Eng Prog 1952;48:89–94.
[16] Miyabe H, Takahashi S, Hamaguchi K. An approach to the design of Stirling ENGINE Regenerator matrix using packs of wire gauzes. Proc IECEC 1982;17:1839–44.
[17] Gedeon D, Wood JG. Oscillating-flow regenerator test rig: hardware and theory with derived correlations for screens and felts. NASA CR-198442; 1996.
[18] Thomas B, Pittman D. Update on the evaluation of different correlations for the flow friction factor and heat transfer of Stirling engine regenerators. American Institute of Aeronautics and Astronautics; 2000.
[19] Tew R et al. Stirling convertor CFD model development and regenerator R&D efforts. NASA TM-213404; 2004.
[20] Ibrahim M, Danila D, Simon TW, et al. Computational modeling of a segmented-involute-foil regenerator for Stirling engines. J Thermophys Heat Transfer 2009;23(4):786–800.
[21] Organ AJ. Thermodynamics and gas dynamics of the Stirling cycle machine. Cambridge University Press; 1992.
[22] Fluent Dynamics Software. ANSYS FLUENT. Lebanon, NT 6.1.7601; 2010.
[23] Dybbs A, Edwards RV. A new look at porous media fluid mechanics – Darcy to turbulent. Fund Transp Porous Media 1984;82:201–56.
[24] Yakhot V, Orszag SA. Renormalization group analysis of turbulence. I. Basic theory. J Sci Comput 1986;1(1):1–51.
[25] Tutar M, Holdo AE. Computational modelling of flow around a circular cylinder in sub-critical flow regime with various turbulence models. Int J Numer Methods Fluids 2001;35:763–84.